Research Article

Morphology and dielectric properties of single sample $Ni_{0.5}Zn_{0.5}Fe_2O_4$ nanoparticles prepared via mechanical alloying

Rafidah HASSAN[a,*], Jumiah HASSAN[a,b], Mansor HASHIM[a,b],
Suriati PAIMAN[a], Raba'ah Syahidah AZIS[a,b]

[a]*Physics Department, Faculty of Science, Universiti Putra Malaysia, 43400 UPM Serdang, Selangor, Malaysia*
[b]*Institute of Advanced Technology, University Putra Malaysia, 43400 UPM Serdang, Selangor, Malaysia*

Abstract: Nickel–zinc ferrite nanoparticles are important soft magnetic materials for high and low frequency device application and good dielectric materials. Nickel–zinc ferrite nanoparticles with composition $Ni_{0.5}Zn_{0.5}Fe_2O_4$ were prepared using mechanical alloying to analyze the effect of sintering temperature on microstructure evolution of a single sample with dielectric properties. The single sample with nanosized pellet was sintered from 600 ℃ to 1200 ℃ and analyzed by X-ray diffraction (XRD) to investigate the phases of the powders and by field emission scanning electron microscopy (FESEM) for the morphology and microstructure analyses. Dielectric properties such as dielectric constant (ε') and dielectric loss (ε'') were studied as functions of frequency and temperature for $Ni_{0.5}Zn_{0.5}Fe_2O_4$. The dielectric properties of the sample were measured using HP 4192A LF impedance analyzer in the low frequency range from 40 Hz to 1 MHz and at temperature ranging from 30 ℃ to 250 ℃. The results showed that single phase $Ni_{0.5}Zn_{0.5}Fe_2O_4$ cannot be formed by milling alone and therefore requires sintering. The crystallization of the ferrite sample increased with increasing sintering temperature, while the porosity decreased and the density and average grain size increased. Evolution of the microstructure resulted in three activation energies of grain growth, where above 850 ℃ there was a rapid grain growth in the microstructure. Dielectric constant and loss factor decreased with the increase in frequency. The optimum sintering temperature of $Ni_{0.5}Zn_{0.5}Fe_2O_4$ was found to be 900 ℃ which had high dielectric constant and low dielectric loss.

Keywords: mechanical alloying; sintering temperature; dielectric properties

1 Introduction

During the past two decades, a much deeper appreciation of solid phenomena has been gained by intensive research into the dielectric properties of materials. One outcome is the present wide range of ferrites which have given rise to new techniques in the overall improvement of communication and computer systems. Dielectric material measurement can provide critical design parameter information for many electronic applications [1]. Nanocrystalline ferrites are important materials because of their electrical, dielectric, magnetic and optical properties which make them suitable for electronic and storage devices. The properties of ferrite materials can be affected by chemical composition and microstructure of the materials which are related to the manufacturing process. The microstructure of ferrite is mainly determined by several factors such as the quality of the

---

* Corresponding author.
E-mail: rafidahhassan89@yahoo.com

raw materials, sintering temperature, milling parameter and sintering condition. Nickel–zinc ferrites are the most popular composition of soft ferrites and the most versatile of all ferrites because of their many technological applications. Ni–Zn ferrites have unique high dielectric constant which enables them to design useful electronic devices and also be used in high frequency applications as core materials for power transformers and circuit inductors in the megahertz frequency region [2].

Ni–Zn ferrites exhibit higher resistivity than Mn–Zn, and are therefore more suitable for frequencies above 1 MHz. They are more stable than the other types of ferrites, easily manufactured and low cost, and have excellent desirable magnetic properties [1]. Dielectric permittivity can be written as $\varepsilon^* = \varepsilon' - j\varepsilon''$, where ε' is the dielectric constant which is the ability of a material to polarize and store a charge within it, whereas the imaginary part ε'' is the loss factor which is a measure of the loss of power usually in the form of heat [3]. Nanoparticles can be synthesized by various physical, chemical and mechanical methods. One of the various techniques for synthesizing the material is mechanical alloying which is used to reduce grain size, mix powder uniformly and produce non-equilibrium structure materials. Mechanical alloying via high energy ball milling has now become one of the conventional methods for producing nano/non-crystalline materials. It is a modified solid state technique used with the advantage of cutting down mixing time. This technique enables economical and rapid preparation of metastable and amorphous alloys, nanocomposites, ceramics and other valuable powders. It is simple and quickly obtained after relatively short laboratory experimentation [4]. During mechanical alloying, materials in powder form will undergo severe collisions between the balls and vial wall of the grinding media by the process of high energy collision that results in a reduction of particle size. The particles themselves which normally possess a distribution of size can be nanoparticles if their average characteristic dimension (diameter for spherical particles) is less than 100 nm. Spinel ferrite nanoparticles have great importance in nanoscience and nanotechnology for technological applications because of their outstanding properties such as nanometer size and large surface area to volume ratio. It has been studied that in Ni–Zn ferrites, the electrical

and magnetic properties of ferrites depend on the stoichiometric composition [5]. The nickel–zinc ferrite with the well known composition of $Ni_{0.5}Zn_{0.5}Fe_2O_4$ is chosen in this study. This composition has high resistivity, good soft magnetic property, low dielectric loss, good mechanical hardness and chemical stability. The study of effect of temperature on structural and dielectric properties is carried out on the sintered Ni–Zn ferrite pellets.

2　Materials and method

The starting raw materials NiO (99.7%), ZnO (99.9%) and Fe_2O_3 (99.7%) with high purity were weighed according to the stoichiometric equation below:

$$0.5NiO + 0.5ZnO + Fe_2O_3 \rightarrow Ni_{0.5}Zn_{0.5}Fe_2O_4$$
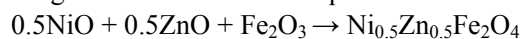
Ferrite nanoparticles $Ni_{0.5}Zn_{0.5}Fe_2O_4$ were prepared by mechanical alloying consisting of a mixture of metallic oxides. The chemicals were mixed with the molar ratio of 0.5:0.5:1 and the ball-to-powder mass-charge ratio (BPR) of 10:1. These compositions were milled for 24 h using a SPEX 8000D high energy ball milling. The initial particle size of the powders was confirmed using transmission electron microscopy (TEM). The powders were mixed with 1–2 wt% polyvinyl alcohol (PVA) as binder and lubricated with 0.3 wt% zinc stearate. The alloyed powders were then uniaxially pressed into a single pellet at a pressure of 4 tonnes to yield a 2.0 g pellet of 18 mm in diameter and 2.0 mm in thickness. A single pellet sample was subjected to repeated sintering process from 600 ℃ to 1000 ℃ at 50 ℃ interval. The sample sintered at different sintering temperature was the same sample. It was sintered for 10 h at the rate of 4 ℃/min. The resulting pellet was used for the characteristic measurement. The sample was examined with X-ray diffraction (XRD, Philips X'pert diffractometer model 7602 EA Almelo) using Cu Kα radiation source with $\lambda = 1.5418$ Å to identify the formed phases. The X-ray powder diffraction pattern was recorded at room temperature in a 2θ scanning range from 20° to 80°.

The field emission scanning electron microscopy (FESEM, FEI NOVA NanoSEM 230) revealed the surface structure of the obtained ferrite and the average grain size was measured by the mean linear intercept method. TEM was carried out on the as-milled powders to confirm the particle size. The density of the sintered pellet for every sintering temperature was

obtained using the Archimedes principle with water as the fluid medium. The theoretical density of $Ni_{0.5}Zn_{0.5}Fe_2O_4$ was calculated by taking its molecular weight to be 237.73 g. The weight of eight molecules in one unit cell is $8 \times 237.73/N_A$ g, where N_A is the Avogadro's number. The volume of a cube with side length a is a^3. The unit cell edge a_0 of $Ni_{0.5}Zn_{0.5}Fe_2O_4$ is 8.3827 Å; therefore $a^3 = 589.0495$ Å^3. As 1 Å^3 = 10^{-24} cm^3, the theoretical density (mass/volume) is equal to 5.3573 g/cm^3. For the dielectric measurements, the Ni–Zn ferrite pellet was sandwiched between two brass electrodes. The dielectric properties of the pellet were determined using Agilent 4294A precision impedance analyzer and carried out in an LT furnace in the frequency range of 40 Hz–1 MHz over the measuring temperature range of 30–250 ℃.

3 Results and discussion

The TEM image of the as-milled raw powders in Fig. 1 shows that the particles are in the nanometer range with particle sizes ranging from 8 nm to 21 nm, and the particles are nearly spherical and agglomerated. The milling time 24 h is chosen because the average grain size can be reduced to less than 100 nm during the milling process due to the high impact of the milling. Mechanical alloying process reaches a steady state when the particles have homogenous shape and size. A steady state is achieved after 30 h milling when there is no change in crystallite size and the size remains constant [6]. There is also a relationship between the temperature of the outer wall and the
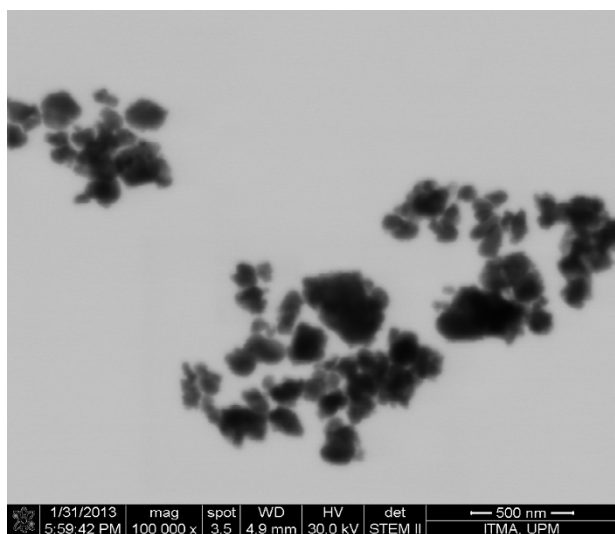
milling time, and the temperature of the vial increases slowly as the milling time is extended. Kinetic energy of the ball and the properties of the material can be controlled by the temperature during the milling process. The diffusivity and the phase transformation caused by milling are also affected by the temperature of the powders. It is assumed that higher temperature results in phases which need higher atomic mobility, while at lower temperature the formation of amorphous phases is expected if the energy is sufficient [7].

The XRD patterns of the $Ni_{0.5}Zn_{0.5}Fe_2O_4$ ferrite nanoparticles are shown in Fig. 2. For the as-milled sample in Fig. 2(a), only raw starting material peaks are observed. The results show that $Ni_{0.5}Zn_{0.5}Fe_2O_4$ could not be formed during milling alone and therefore requires sintering, suggesting that the thermal energy should be supplied to the materials during the sintering process to complete the reaction. In ceramics, sintering is always an important processing parameter that
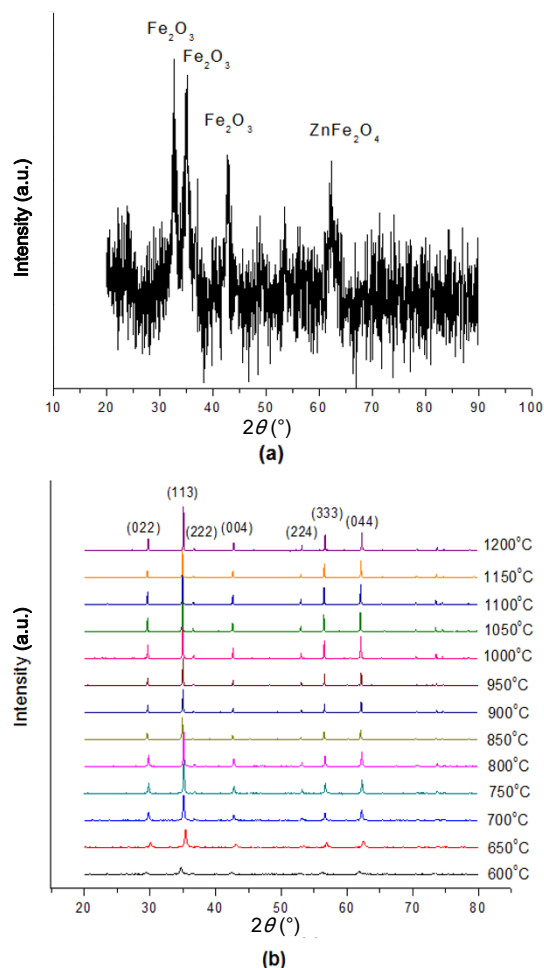

Fig. 1   TEM image of the as-milled raw powders.

Fig. 2   (a) XRD pattern of the as-milled powders; (b) XRD spectra of $Ni_{0.5}Zn_{0.5}Fe_2O_4$ after sintering from 600 ℃ to 1200 ℃.

influences ceramics' microstructure evolution, grain growth and densification [8]. As shown in Fig. 2(b), when the sample is sintered at 600 ℃, the single phase crystallization of $Ni_{0.5}Zn_{0.5}Fe_2O_4$ is detected indicating the formation of nickel–zinc ferrite. All peaks match the standard pattern of nickel–zinc ferrite 00-008-0234 of the ICDD database that shows $Ni_{0.5}Zn_{0.5}Fe_2O_4$ and can be clearly indexed to the seven major peaks of the spinel ferrites, which are (022), (113), (222), (004), (224), (333) and (044) planes of a cubic unit cell, corresponding to spinel structure. It confirms that the single sample sintered Ni–Zn ferrite has single phase cubic spinel structure and the entire peaks observed match well with those of Ni–Zn ferrites. The full crystallization is achieved at as low as 600 ℃ exhibiting the advantage of mechanical alloying. Moreover, the major change observed is the increment in the intensity of the ferrite sample as the sintering temperature increases. The increase in the intensity means that either the contents of the phases are increased or the concentration of the atoms in the alloy is higher. All the XRD peaks become sharper and narrower with increase in temperature. This indicates the increase in particle size and the enhancement of crystallinity.

It also shows the relationship of porosity and density with sintering temperature in Table 1. The results obtained reveal a linear increase in density with sintering temperature. It is found that there is more densification or less porosity at the higher sintering temperature. The true porosity of the sample is calculated using X-ray density, and the density increases while porosity decreases with sintering temperature. This is because both porosity and density are inversely proportional to each other and are fractions of theoretical density of the material. The sintered density of the sample is between 4.575 g/cm^3 and 5.179 g/cm^3 or about 86%–97% of the theoretical density of 5.3573 g/cm^3. The sintering of the nanocrystalline material influences the particle size, shape and crystallization. The total pores are directly related to the density. Therefore higher heat treatment is required to remove a fraction of the pores. Sintering is the control of both densification and grain growth as densification is the act of reducing porosity in the sample thereby making it denser and thus changing the pore structure which affects ferrite properties.

The FESEM micrographs and the process of grain growth are taken on the surface microstructure of

Table 1   Average grain size, porosity and measured density of $Ni_{0.5}Zn_{0.5}Fe_2O_4$

Sintering temperature (℃)	Measured density (g/cm^3)	Theoretical density (%)	Porosity (%)	Average grain size (nm)
600	4.575	85.878	14.121	88.479
650	4.659	87.455	12.545	89.697
700	4.666	87.587	12.413	100.578
750	4.718	88.562	11.437	101.316
800	4.740	88.976	11.024	103.755
850	4.828	90.628	9.372	114.202
900	4.868	91.378	8.622	120.282
950	4.879	91.585	8.415	162.777
1000	4.896	91.904	8.096	188.845
1050	4.925	92.448	7.552	215.061
1100	4.966	93.218	6.782	239.727
1150	5.066	95.095	4.905	453.838
1200	5.179	97.216	2.784	645.744

sintered $Ni_{0.5}Zn_{0.5}Fe_2O_4$ with sintering temperature from 600 ℃ to 1200 ℃ by using a scanning electron microscope as shown in Fig. 3. The average grain size of a sintered body is measured over 200 grains by the linear intercept method. From Table 1, it is found that the average grain size increases with sintering temperature and it shows the microstructure evolution of the sample. The densification rate decreases as the distance of the defects to the grain boundaries increases with increasing grain size. Grain growth also gives pore coalescence where smaller pores are merged together into larger ones and this also reduces the densification rate and explains the density results obtained. The increasing average grain size may be due to mass transport mechanism in the sample during the sintering process. Sintering could be defined as removal of the pores between starting particles combined with grain and formation of strong bonds between adjacent particles. Thermal energy provided by increasing sintering temperature makes the particles move closer, thus contributing to the initial stage of grain growth. It is obviously seen that there is inhomogeneity in the microstructure that shows big size pores meaning that probably only a few crystallite sizes are present in the bulk sample. At initial sintering temperature of 600–750 ℃, it involves rearrangement of the powder particles and formation of strong bonds or necks at the contact points between particles. At intermediate sintering temperature from 800 ℃ to 1075 ℃ where the size of the necks grows, the amount of porosity decreases and particles move closer. The final stage of sintering at 1100 ℃, 1150 ℃ and 1200 ℃

exhibits that the pores are spherical and closed, removed slowly by diffusion process of pore vacancies and significant grain growth is clearly seen at this stage. As the sintering temperature increases, the driving force promoting neck growth increases [9]. Neck growth among the grains contributes to the increase in the average grain size.
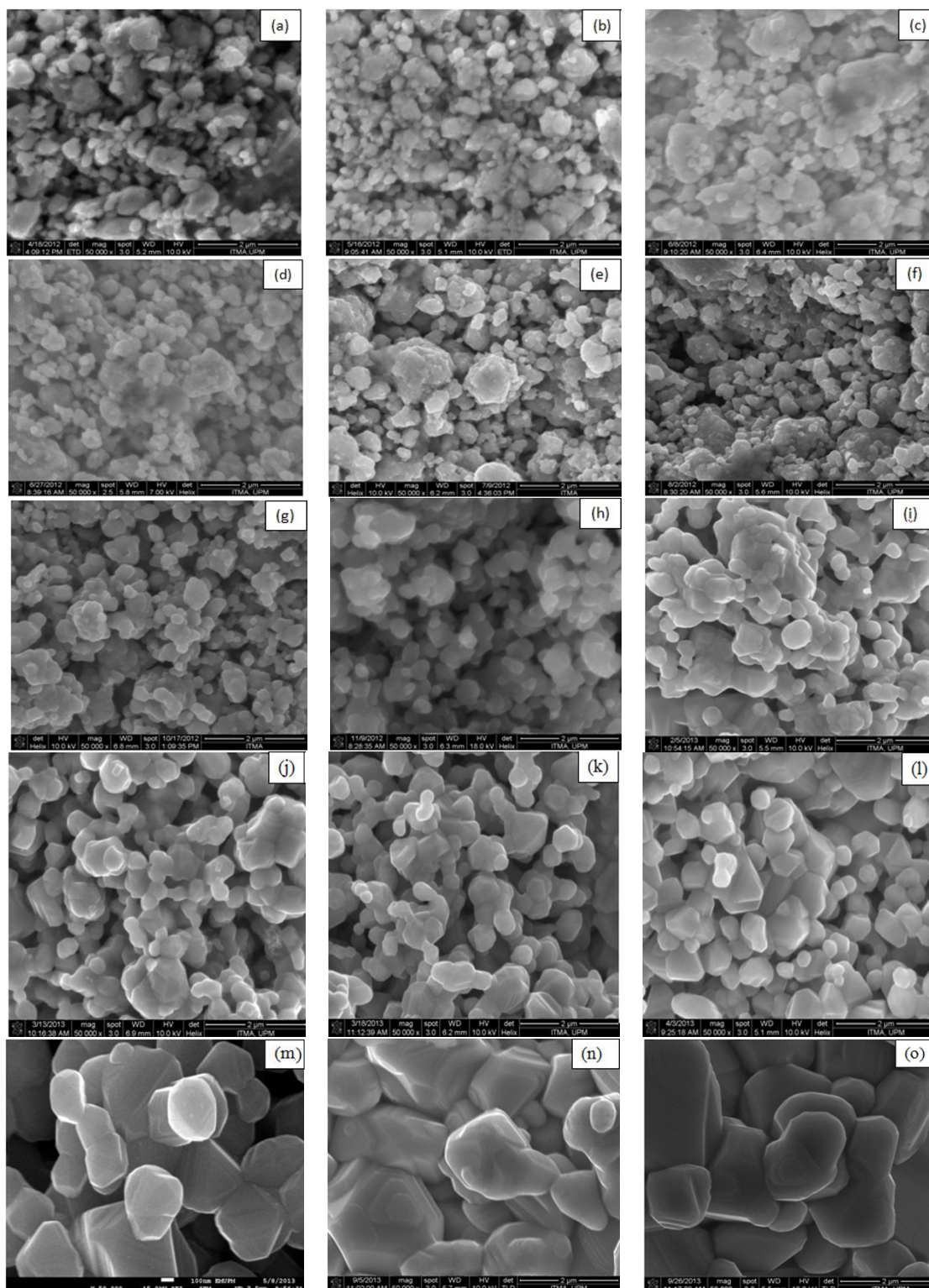

Fig. 3   SEM images of $Ni_{0.5}Zn_{0.5}Fe_2O_4$ at different sintering temperatures: (a) 600 ℃, (b) 650 ℃, (c) 700 ℃, (d) 750 ℃, (e) 800 ℃, (f) 850 ℃, (g) 900 ℃, (h) 950 ℃, (i) 1000 ℃, (j) 1025 ℃, (k) 1050 ℃, (l) 1075 ℃, (m) 1100 ℃, (n) 1150 ℃ and (o) 1200 ℃.

Table 1 shows the average grain size, porosity and measured density of the sample. The X-ray density and porosity listed in Table 1 are obtained by using Eqs. (1) and (2), respectively:

$$p_{xrd} = 8M / (N_A a^3) \qquad (1)$$

where p_{xrd} is the X-ray density; M is the molecular weight of the sample; N_A is the Avogadro's number; and a is the lattice constant. The porosity (P) of the sample is calculated by using the equation:

$$P = (1 - p_{exp} / p_{xrd}) \times 100\% \qquad (2)$$

where p_{exp} is the experimental density determined from the Archimedes principle. The theoretical density for $Ni_{0.5}Zn_{0.5}Fe_2O_4$ is 5.3573 g/cm^3.

The activation energy for grain growth can be predicted from the behavior of particle growth by using the Arrhenius equation below [10]:

$$d \ln k / dT = Q / (RT^2) \qquad (3)$$

where k is the specific reaction rate constant; Q is the activation energy; T is the absolute temperature; and R is the ideal gas constant. The value of k can be directly related to grain size [9], which results in the equation:

$$\log D = (-Q / 2.303R) \times 1 / T \qquad (4)$$

where T is the absolute temperature and D is the grain size. From Eq. (4), there are three best fitted straight-line plots of grain size where $\log D$ versus $1/T$ is shown in Fig. 4. Three slopes of the line are also obtained which are y_1, y_2 and y_3 of $-Q / 2.303R$, and the value of the activation energies of grain growth Q can be calculated from the Arrhenius plots of y_1, y_2 and y_3 which are 4.56 kJ/mol, 27.94 kJ/mol and 109.139 kJ/mol, respectively. The activation energies are increasing with rise in sintering temperature as the average grain size is increased from nano size to micron size where the grain growth is depending on pore removal that
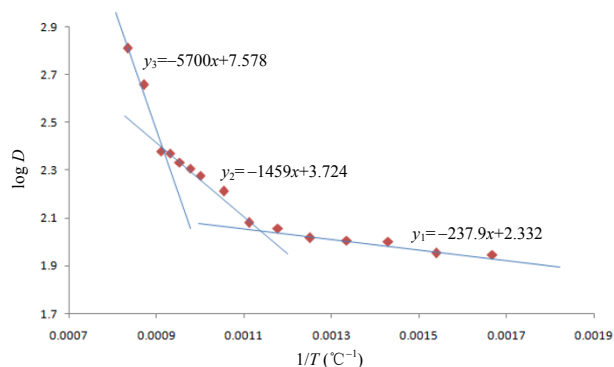

Fig. 4   Arrhenius plot of activation energies for grain growth of $Ni_{0.5}Zn_{0.5}Fe_2O_4$.

supports the view that a metastable network of pores and boundaries occurs especially in the intermediate and final stages of sintering. All of these values are much lower than that reported by previous researcher [11] where the average grain size of Ni–Zn ferrites at different sintering temperatures is larger and also lower than that obtained by Rao *et al*. for Ni–Zn ferrites prepared using conventional ceramic method [12]. The low activation energies are due to the smaller size of starting powders milled by the mechanical alloying that reduces their dimensions into the nanosized range. This causes the surface area of the starting powders to be increased and lowers the activation energy. Higher activation energy is required in order to continue the growth of grains which is the result of atom diffusion in grain boundary and an energy barrier that must be overcome for a reaction to occur. Furthermore, the sample has been sintered repeatedly, causing it to have a thermal history and higher activation energy required for the further stage of the grain growth. The rates controlling transport mechanism for densification, grain growth and coarsening have different activation energies and hence dominate in different temperature regimes. In general, the coarsening mechanism dominates at lower temperature due to lower activation energy. The heating rate of sintering is controlled to maintain a constant densification rate. In constant heating rate, contribution from surface diffusion is minimized since the time of surface diffusion regime is comparatively small.

The dielectric properties ε' and ε'' in the frequency range 40 Hz–1 MHz with measuring temperature from 30 ℃ to 250 ℃ at each sintering temperature are illustrated in Figs. 5 and 6, respectively. Both ε' and ε'' curves for all the samples sintered at 600–1000 ℃ show similar trends, decreasing with increasing frequency. This decrease is rapid at lower frequency and becomes slower at higher frequency which is a normal dielectric behavior in ferrites having mobile charge carriers. In Fig. 5, the dielectric dispersion curve and the decrease observed at lower frequency region can be explained on the basis of Koop's phenomenological theory [13] due to Maxwell–Wagner interfacial type of polarization [14]. The dispersion of ε' at low frequency is due to the interfacial polarization and existence of depletion layers near the sample–electrode contacts. It is assumed that there should be two layers which are well

conducting materials (ferrite grains) and separated by the layers of lower conductivity (grain boundaries) that are effective at higher and lower frequencies respectively in the inhomogeneous dielectric structure. It can be also explained on the basis of space charge polarization resulted from difference among the conductivities of the various phases present. At low frequency electron hopping occurs between Fe^{3+} and Fe^{2+} on the localized sites. The electrons attain the grain boundary through hopping of charge carriers which results in the interfacial polarization. However, as the frequency is increased, the probability of electrons reaching the grain boundary decreases, which results in a decrease in the interfacial polarization. Therefore, the dielectric constant decreases with increasing frequency. Besides this, the sintered ferrite material consists of cracks, pores and other defects, and due to inhomogeneity, there are regions of different permittivity. Thus the conducting grains and less conducting boundaries are separated by voids or pores which were explained by Maxwell and Wagner.

The sample shows high values of ε' for frequencies lower than 10^3 Hz, but at high frequencies (10^3–10^6 Hz) as the temperature increases ε' decreases. At low frequencies the charges have time to accumulate at the borders of the conducting regions causing ε' to increase, while at higher frequencies the charges do not have time to accumulate and polarization does not occur since the charge displacement is small compared to the dimensions of the conducting region [15]. When orientational polarization is dominated in the system, the temperature randomizes it and tends to decrease the dielectric constant. Therefore, the overall dielectric constant is going to decrease in the system. However, if polarization is predominantly governed by the space polarization then dielectric constant of the system is going to increase with increasing temperature because the rate of interfacial charge accumulation increases. As a result, the present sample exhibits the orientational polarization predominantly. At low frequencies, the dielectric constant is mainly due to the movement of free charges which increases with the rise in temperature and further increases the value of dielectric constant. But at high frequencies and high temperature, dispersion losses increase due to the thermal vibrations and less time is available for the material to respond to the applied electric field. The rapid increase in the dielectric constant with increase

in temperature at low frequency suggests that the effect of temperature is more pronounced on the interfacial polarization rather than on the dipolar polarization. The electron exchanges between the ferrous and ferric ions, which produce local displacements in the direction of the applied external fields, determine the polarization in ferrites. Above certain frequencies of the electric field, this electronic exchange cannot follow the alternating field and this causes a decrease in the dielectric constant.

From the graphs, the dielectric constant initially increases gradually with temperature at lower frequency of 100 Hz and then it begins to decrease at 1 kHz to 1 MHz, but up to particular measuring temperature 250 ℃, it becomes constant and slowly decreases. This is attributed to the transition of the sample due to a magnetic transition from ferromagnetic to paramagnetic that changes the behavior of the dielectric constant with temperature. A further increase in temperature adds to the random vibrational motion of the molecules, which becomes less susceptible to the orientation in the field direction and hence the dielectric constant decreases. The space charge polarization resulting from electron displacement on application of electric field and the following charge build up at the insulating grain boundary is a major contributor to the dielectric constant in ferrites. Space charge polarization is expected when there are large numbers of Fe^{2+} ions in the ferrite. It is due to the ease of electron transfer between Fe^{3+} and Fe^{2+} ions and consequently higher dielectric constant. Now, with increasing sintering temperature, partial reduction of Fe^{3+} to Fe^{2+} takes place. Thus, the value of dielectric constant increases with increasing sintering temperature.

The dielectric loss factor decreases with increasing frequency and increases with temperature from 30 ℃ to 250 ℃ as shown in Fig. 6. The frequency and temperature effects on the ε'' illustrate the interfacial polarization of the grain boundaries within the sample. These frequency and temperature dependences are due to the conversion of the movement of phonons into the vibrations of the lattice. The inconsistent lattice vibrations cause instability in the interfacial polarization. Therefore, ε'' increases. For the lower frequency, the polarization is increased by the electric field and also by the increase in the number of charge carriers with increasing temperature. Dielectric loss in ferrites is also a result of the lag in polarization with
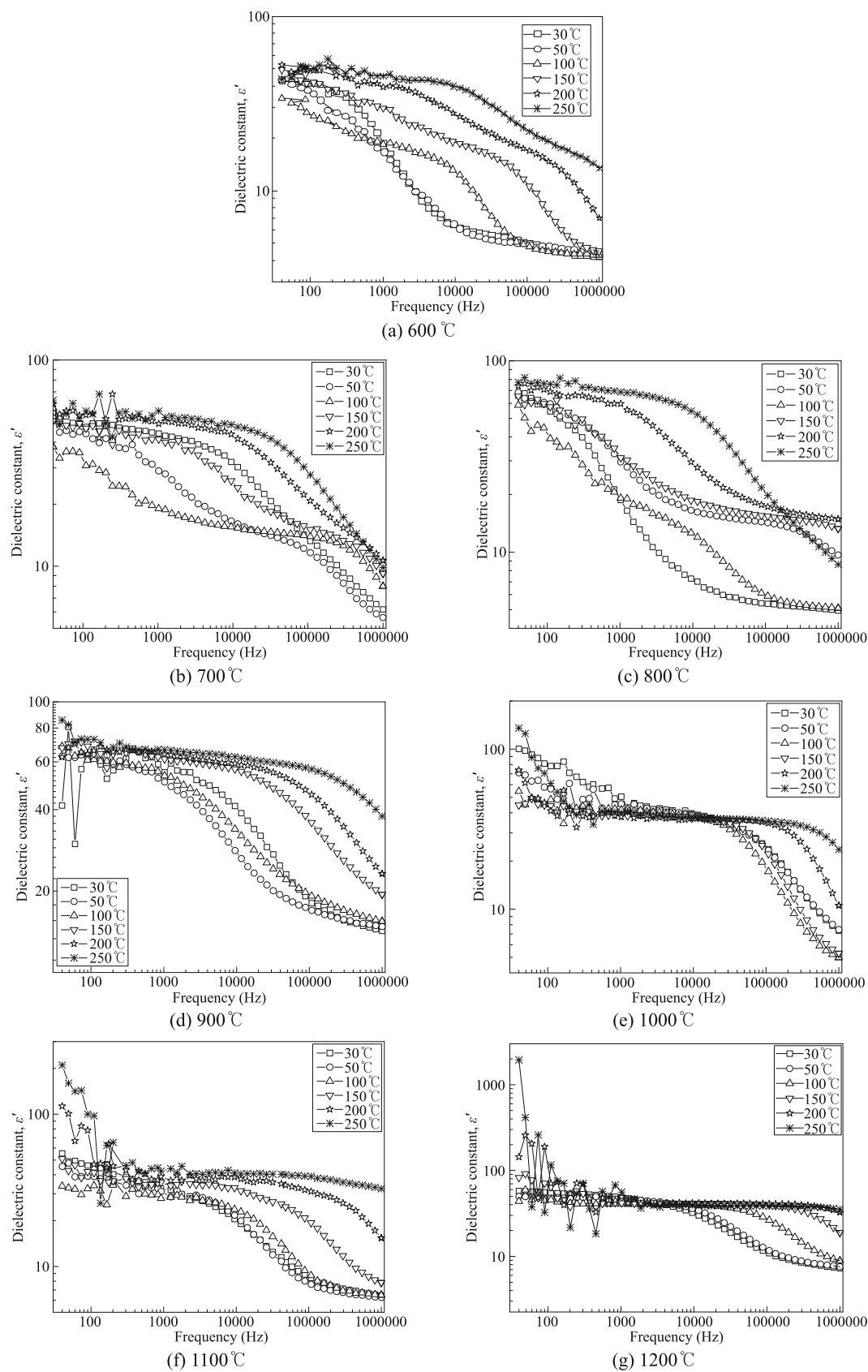
Fig. 5 Dielectric constant of $Ni_{0.5}Zn_{0.5}Fe_2O_4$ sintered at different temperatures: (a) 600 ℃, (b) 700 ℃, (c) 800 ℃, (d) 900 ℃, (e) 1000 ℃, (f) 1100 ℃ and (g) 1200 ℃.

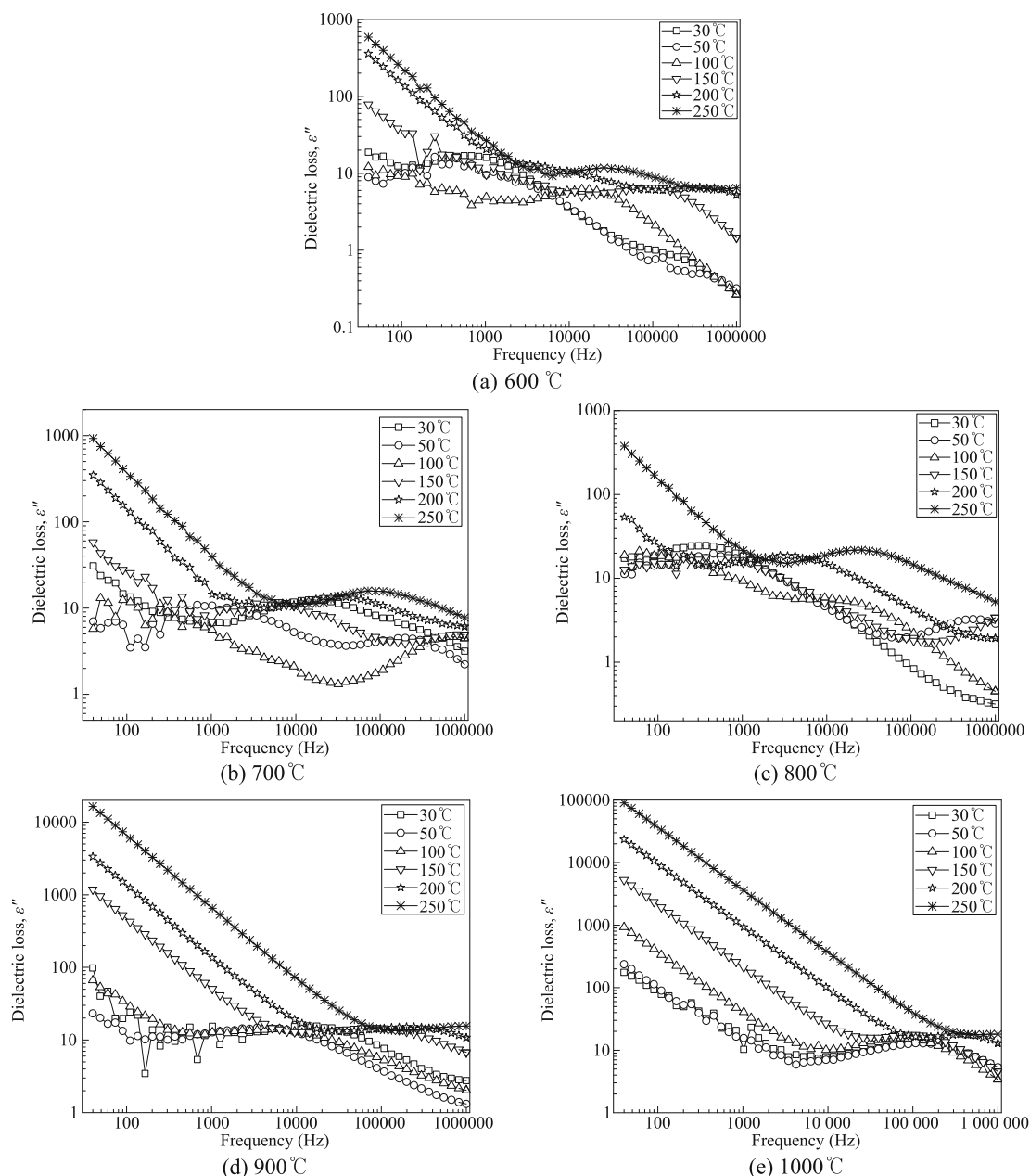Fig. 6　Dielectric loss factor of $Ni_{0.5}Zn_{0.5}Fe_2O_4$ sintered at different temperatures: (a) 600 ℃, (b) 700 ℃, (c) 800 ℃, (d) 900 ℃ and (e) 1000 ℃.

respect to the applied alternating electric field. When the frequency of the external AC field is equal to the hopping frequency of the charge carriers, the maximum electrical energy is transferred to the oscillating ions and we observe that there are broad peaks in power loss. A broad peak of ε'' indicates the occurrence of distribution of relaxation time rather than a single relaxation time [16]. The increment of ε'' is low from 30 ℃ to 250 ℃ especially at higher frequency. The atoms or molecules in the sample

cannot in most cases orient themselves in the low temperature region. As the temperature rises, the orientation of the dipoles is facilitated and this increases the permittivity. When the frequency of applied AC field is much larger than the hopping frequency of electrons, the electrons do not have an opportunity to jump at all and the energy loss is small. In general, the local displacements of electronic charge carriers cause the dielectric polarization in materials. Therefore the marked decrease in ε'' is due to the

decreasing ability of the jumping electrons to follow the alternating frequency of AC electric field beyond certain critical frequency. This explains the decreasing trends for ε'' with increasing frequency. As observed from the graphs, the decrement of ε'' is very rapid at higher temperature in low frequency region, but at frequency 1 kHz and above it decays with slow rate reaching a constant value at high frequencies and low temperature. This proposes a thermally activated hopping process with increasing temperature at low frequencies.

$Ni_{0.5}Zn_{0.5}Fe_2O_4$ sintered at low temperature has the lowest dielectric constant. This may be due to the incomplete phase formation and low crystallization of $Ni_{0.5}Zn_{0.5}Fe_2O_4$. Another reason may be the agglomerations of powders bonded with grains as mentioned above. Agglomerations of powders become a resistant for ions to polarize between grains and grain boundaries [17]. ε' and ε'' increase with increasing temperature which is normally an expected behavior that has been observed in most of the ferrites. The hopping of charge carriers is thermally activated with the temperature rise, and hence the dielectric polarization increases causing an increase in ε' and ε'' with temperature. High temperature sintering also leads to the escape of Zn^{2+} ions from the lattice, which results in greater structural imperfections and high dielectric loss. From the SEM images, the neck growth among the grains increases as sintering temperature increases. On the other hand, dielectric constant of the sample also possesses the phenomena. Polarization of ions in grains may increase with grain necking growth. Polarization of ions in grains is the main factor that influences the dielectric constant. The grain size increases, but the porosity decreases with increasing sintering temperature. The increase in the grain size decreases the grain boundary density between them. The sample becomes denser and more homogenous. Low porosity, high density and increasing grain size increase the dielectric permittivity. It is found that higher temperature which reduces pores can cause the larger dielectric constant ε' at low frequency which is due to the blocking of charge carriers at the electrodes. Space charge polarization induces the dispersion of ε' because the enhanced mobility of charge carriers increases as the temperature increases which is thermally generated from the beginning resulting in an increase of ε'.

4 Conclusions

A single sample of $Ni_{0.5}Zn_{0.5}Fe_2O_4$ ferrite nanoparticles was successfully synthesized via high energy ball milling and the parallel evolutions of dielectric and microstructural properties were obtained. High energy ball milling is an effective technique to improve the preparation of Ni–Zn ferrite nanoparticles at lower temperatures. The particles are in the nanometer size of around 22 nm in average. The effect of increasing sintering temperature changes the microstructure of the material, leading to the changes in the dielectric properties of the material. The results show that single phase $Ni_{0.5}Zn_{0.5}Fe_2O_4$ could not be formed during milling alone and therefore requires sintering. The crystallization of the ferrite increases with increasing sintering temperature, which decreases the porosity and increases the density and crystallite size. The activation energies of grain growth (Q) are 4.56 kJ/mol, 27.94 kJ/mol and 109.139 kJ/mol where the rate of grain growth is slower initially from 600 ℃ to 850 ℃ but grows rapidly at higher sintering temperature above 850 ℃. The sintered density of the sample was between 4.575 g/cm^3 and 5.179 g/cm^3 or about 86%–97% of the theoretical density of 5.3573 g/cm^3. Both ε' and ε'' decrease with increasing frequency, which is a normal dielectric behavior in ferrites. The optimum sintering temperature having the highest dielectric constant and the lowest dielectric loss factor, which are 14.22 and 2.762 respectively, is 900 ℃.

References

[1] Agilent Technologies. Agilent solutions for measuring permittivity and permeability with LCR

meters and impedance analyzers. Application Note 1369-1. 2006. Available at http://cp.literature.agilent.com/litweb/pdf/5980-2862EN.pdf.

[2] Matsushita N, Kondo K, Yoshida S, *et al*. Ni–Zn ferrite films synthesized from aqueous solution usable for sheet-type conducted noise suppressors in GHz range. *J Electroceram* 2006, **16**: 557–560.

[3] Hassan J, Yen, FM, Hashim M, *et al*. Dielectric permittivity of nickel ferrites at microwave frequencies 1 MHz to 1.8 GHz. *Ionics* 2007, **13**: 219–222.

[4] Verma A, Chatterjee R. Effect of zinc concentration on the structural, electrical and magnetic properties of mixed Mn–Zn and Ni–Zn ferrites synthesized by the citrate precursor technique. *J Magn Magn Mater* 2006, **306**: 313–320.

[5] Mangalaraja RV, Anathakumar S, Manohar P, *et al*. Magnetic, electrical and dielectric behaviour of $Ni_{0.8}Zn_{0.2}Fe_2O_4$ prepared through flash combustion technique. *J Magn Magn Mater* 2002, **253**: 56–64.

[6] Ismayadi I, Hashim M, Khamirul AM, *et al*. The effect of milling time on $Ni_{0.5}Zn_{0.5}Fe_2O_4$ compositional evolution and particle size distribution. *Am J Applied Sci* 2009, **6**: 1548–1552.

[7] El-Eskandarany MS, Sumiyama K, Suzuki K. Crystalline-to-amorphous phase transformation in mechanically alloyed $Fe_{50}W_{50}$ powders. *Acta Mater* 1997, **45**: 1175–1187.

[8] Rahman MN. *Ceramic Processing and Sintering*, 2nd edn. CRC Press, 2003.

[9] German RM. *Sintering Theory and Practice*. John Wiley & Sons Inc., 1996.

[10] Coble RL. Sintering crystalline solids. I. Intermediate and final state diffusion models. *J Appl Phys* 1961, **32**: 787–792.

[11] Ismail I, Hashim M. Structural and magnetic properties evolution of fine-grained $Ni_{0.5}Zn_{0.5}Fe_2O_4$ series synthesized via mechanical alloying. *Australian Journal of Basic and Applied Sciences* 2011, **5**: 1865–1877.

[12] Rao BP, Rao PSVS, Rao KH. Densification, grain growth and microstructure of Ni–Zn ferrites. *J Phys IV France* 1997, **07**: C1-241–C1-242.

[13] Koops CG. On the dispersion of resistivity and dielectric constant of some semiconductors at audiofrequencies. *Phys Rev* 1951, **83**: 121.

[14] Wagner KW. Zur theorie der unvollkommenen dielektrika. *Annalen der Physik* 1913, **345**: 817–855.

[15] Maxwell JC. *A Treatise on Electricity and Magnetism, Vol. 1*. New York: Oxford University Press, 1973: 828.

[16] Olofa SA. Oscillographic study of the dielectric polarization of Cu-doped NiZn ferrite. *J Magn Magn Mater* 1994, **131**: 103–106.

[17] Jonscher AK. *Dielectric Relaxation in Solids*. London: Chelsea Dielectrics Press, 1983: 231.